Interspecies Variation in Biodistribution of Technetium (2-Carbomethoxy-2-Isocyanopropane)$_6^+$

James F. Kronauge, Michael A. Noska, Alan Davison, B. Leonard Holman, and Alun G. Jones

The Joint Program in Nuclear Medicine, Harvard Medical School, and Brigham and Women's Hospital, Department of Radiology, Boston, Massachusetts and Department of Chemistry, Massachusetts Institute of Technology, Cambridge, Massachusetts

The cationic complex technetium (2-carbomethoxy-2-isocy-anopropane)$_6^+$ (^{99m}Tc-CPI) contains terminal ester groups that were included to provide a pathway for in-vivo metabolism of this compound, thereby enhancing its performance as a myocardial perfusion agent. Biodistribution studies of the compound demonstrated myocardial accumulation in rabbit, guinea pig, and chick, but not in rat and mouse. Radiochemical analysis by HPLC after in-vitro incubation of ^{99m}Tc-CPI in blood plasma from the various species confirmed enzymatic hydrolysis to numerous new compounds. Rat and mouse serum produced complete hydrolysis of this agent after incubation for less than 5 sec at 25°C or rates greater than 500 times those observed in human, rabbit, guinea pig and chick serum. Chemical synthesis and isolation of the monohy-drolyzed species with subsequent biodistribution studies in guinea pig and rabbit confirmed that this neutral lipophilic complex did not accumulate in heart tissue. It is concluded that varying rates of enzymatic in-vivo hydrolysis produce the interspecies biodistribution differences and may account for the moderate myocardial clearance relative to other isonitrile complexes.

J Nucl Med 1992; 33:1357–1365

Interspecies variation in biodistribution has long plagued the development of radiopharmaceuticals, especially in the discovery of technetium heart (*1,2*) and brain perfusion agents (*3*). No single animal is an acceptable model for humans; therefore, validating preclinical biodistribution studies is an important step before proceeding to clinical trials. Evaluation of the biodistribution of a compound alone, when the biochemical mechanisms for localization or the pharmacokinetics are unknown, reduces nuclear medicine to the simple visualization of anatomy. Empirically obtained biodistribution data should also include radiochemical analysis as a test for metabolism or decom-

position in vivo. This validation of the chemical integrity of a radiopharmaceutical in vivo becomes especially important with the less stable (*4*) or biologically reactive functionalities of the newer agents (*5–10*).

The first technetium heart agent to be successful in humans, technetium (t-butyl isocyanide)$_6^+$ [^{99m}Tc-TBI] (*11*), exhibited high myocardial extraction, but slow clearance from the lungs back into the blood as well as very high uptake and prolonged retention in the liver (*12*). The structurally similar compound technetium (2-carbome-thoxy-2-isocyanopropane)$_6^+$ [^{99m}Tc-CPI] is also a lipophilic cationic complex containing six identical functionalized isonitrile ligands (*10*). The terminal methyl ester functions on the ligands were included in the design of this molecule to introduce an unstable organic functional group that could undergo metabolism or decomposition thus enhancing biologic excretion after initial myocardial extraction had occurred.

Preliminary screening of ^{99m}Tc-CPI in rabbit demonstrated high initial accumulation of activity in the heart, liver and kidney with rapid clearance from blood and lung, followed by moderate hepatobiliary and renal clearance and more gradual myocardial washout (*13*). During toxicologic and preclinical dosimetry evaluations of ^{99m}Tc-CPI kit formulations in other species, however, distinct differences in biodistribution were observed in that no myocardial accumulation was observed in rat or mouse (*14*). Further screening in other species along with pharmacologic evaluation of the compound's radiochemical integrity were performed to ascertain the nature of these differences and to determine the ability of the guinea pig model to predict the behavior of an agent in human.

MATERIALS AND METHODS

The metastable radionuclide ^{99m}Tc, as sodium pertechnetate (30-150 mCi/ml, 1.1–5.5 GBq/ml), was obtained from a commercial ^{99}Mo/^{99m}Tc generator (DuPont/Biomedical Products, N. Billerica, MA). Synthesis and characterization of CPI, the ^{99}Tc(CPI)$_6^+$ complex and ^{99m}Tc-TBI have been published elsewhere (*10,15*).

Chromatography

Reversed-phase thin-layer chromatography (RP-TLC) was performed on Whatman MK C-18 plates developed in methanol/acetonitrile/tetrahydrofuran/aqueous buffer (ammonium acetate, 0.5 M) (3:3:2:2, v:v:v:v). High-performance liquid chromatography (HPLC) was carried out on a sequential dual-detector system, uv-vis (254 nm) and NaI-based radiometric detection (Waters Associates, Woburn, MA) as described previously (16). Analytical HPLC analysis of ^{99m}Tc-CPI and its metabolites was accomplished in a reversed-phase mode (RP-HPLC) with a C$_8$ bonded (5 μM) spherical silica particle stationary phase (Brownlee OS-MP cartridge, 100 mm × 4.1 mm) (Rainin Instruments, Woburn MA) and a gradient mobile phase of 100% aqueous buffer (ammonium sulfate, 0.05 M, pH 5.5) to 95% methanol in a 5-min linear gradient at a flow rate of 1 ml/min.

Biological samples were made ready for RP-HPLC analysis using a pre-wet (C-18) Sep-Pak Cartridge (Waters, Milford MA) prepared by first injecting, via a syringe through the cartridge, absolute ethanol (5 ml) followed by distilled water (5 ml) and finally air (10 ml).

Radiochemical Preparations

Technetium-99m-CPI was synthesized by addition of ^{99m}TcO$_4^-$ (20-200 mCi, 0.74-7.4 GBq, 1-2 ml 0.15 M saline) to a vial containing sodium dithionite (5.0 mg, 0.029 mmol), ethanol (0.25 ml, 95%) and the liquid CPI ligand (5 μl, 0.039 mmol) followed by heating at 65°C for 30 min. Separation of the radiolabeled complex from reagents was performed by loading the cooled solution (1.0 ml) onto a pre-wet C-18 Sep-Pak and flushing the cartridge with saline (0.15 M, 10 ml) followed by ethanol/water (30%, 5 ml) and ethanol/saline (95%, 5 ml). Radiochemical purity was determined by both RP-HPLC and RP-ITLC to be >95% and stable for more than 6 hr. The identity of the ^{99m}Tc-CPI species was confirmed by RP-HPLC with the characterized ^{99m}Tc(CPI)$_6^+$ and a retention time of 9.0 min (k' = 4.30); RP-TLC R$_f$ = 0.7.

Preparation of the First Hydrolysis Product of ^{99m}Tc-CPI

The neutral monohydrolyzed product of the cationic ^{99m}Tc-CPI complex [Tc(CNC(CH$_3$)$_2$COOCH$_3$)$_5$(CNC(CH$_3$)$_2$COO$^-$)]°, [Tc(CPI)$_5$(H-CPI)]°, was synthesized by incubating the reconstituted ^{99m}Tc-CPI preparation at pH 9.0 for 10 min at 25°C followed by neutralization to pH 6.0 with HCl (0.5 M). The solution (100 mCi, 3.7 GBq/ml) was loaded onto a C-18 Sep-Pak, and the cartridge was eluted with ethanol/saline (30%, 5 ml) followed by ethanol/water (90%, 5 ml) to isolate the neutral lipophilic complex in an overall 5% yield. The RP-HPLC retention time was 8.2 min (k' = 3.8); RP-TLC R$_f$ = 0.6.

Animal Biodistribution

Albino rats (male CD, 400-650 g) and albino mice (male CD-1, 25-35 g) were obtained from Charles River Breeding Laboratories, Wilmington, MA; male Hartley guinea pigs (300-600 g) from Elm Hill, Chelmsford, MA; and 4-day-old Leghorn chicks (40-60 g) (SPF-utility chicks) from Spafas, Norwich, CT. New Zealand albino rabbits (3-4 kg) were purchased from Pine Acre Rabbitry, Assonet, MA.

Dynamic gamma camera imaging studies were performed after i.v. injection of ^{99m}Tc-CPI (1.0 mCi, 37 MBq/0.2 ml) under sodium pentobarbital anesthesia. Images were collected on a LEAP collimated GE 400T gamma camera (GE Medical Systems,

Milwaukee, WI) at 60-sec intervals for 1 hr in a 64 × 64 matrix. Time-activity curves for heart, lung, liver and kidney were obtained without background subtraction.

Quantitative biodistribution studies were performed in mice, rats, guinea pigs and 5-day-old chicks. Unanesthetized mice were injected with ^{99m}Tc-CPI (25 μCi, 0.9 MBq/100 μl) via a tail vein and killed by cervical dislocation. Rats and guinea pigs under i.p. sodium pentobarbital anesthesia (35-50 mg/kg body weight) were administered ^{99m}Tc-CPI (100 μCi, 3.7 MBq/100 μl) via an exposed femoral vein and killed by cardiac puncture. Unanesthetized chicks were injected with ^{99m}Tc-CPI (25 μCi, 0.9 MBq/100μl) via a wing vein and killed by ether asphyxiation.

In-Vitro Hydrolysis of ^{99m}Tc-CPI

In-vitro hydrolysis of the radiolabeled compound was examined using plasma from freshly drawn heparinized blood. Human blood was obtained from fasted (>8 hr), healthy male and female volunteers, with normal HDL, LDL and triglyceride levels. For interspecies comparison, heparinized blood was taken by cardiac puncture from ether-anesthetized male albino guinea pigs, mice and rats and from unanesthetized rabbits via an ear vein. Blood samples were centrifuged at 3000 × g for 5 min to separate cells, and the plasma was kept cold (4°C) until use. In each hydrolysis experiment, plasma (0.20 ml) was pipetted into a borosilicate culture tube and equilibrated to 37°C in a water bath. The ^{99m}Tc-CPI complex (10-50 mCi/ml, 0.37-1.85 GBq/ml, 20 μl) was added, the contents were shaken and incubation was continued for various periods of time. Enzymatic hydrolysis was halted by the addition of cold (4°C) absolute ethanol (1.0 ml) and cooling in an ice bath to precipitate serum proteins. The samples were centrifuged (15 min, 2500 × g, 4°C) and the supernatant was analyzed by RP-HPLC. Repeated RP-HPLC analysis on the same sample demonstrated that further hydrolysis did not occur in the ethanolic supernatant.

RESULTS

Biodistribution Studies

Dynamic gamma camera studies in rabbits provided a simple direct comparison of pharmacokinetics for different technetium compounds. Figure 1A shows a rabbit whole-body image obtained 60 min postinjection of ^{99m}Tc-TBI, which served as our relative standard. Distinct visualization of the heart is made just above the persistently hot liver. Time-activity curves for this agent (Fig. 1B) show the high initial lung uptake with gradual clearance that obscures visualization of the heart until 20 min postinjection when the heart-to-lung ratio exceeds 2. Dynamic gamma camera imaging of ^{99m}Tc-CPI in the same species (Fig. 2A) also reveals good visualization of the heart; however, as appreciated in the time-activity curves, resolution of the heart from background lung activity occurred much earlier in the study due to the lower initial pulmonary accumulation and more rapid clearance (Fig. 2B). Blood activity, measured by venous sampling from the ear opposite that of injection, showed very rapid clearance to 0.04% per gram by 5 min postinjection. Thus, greater than 95% of the heart-associated activity reflects retention within the myocardium. The conspicuous donut can be observed in the high-resolution image shown in Figure 2C,
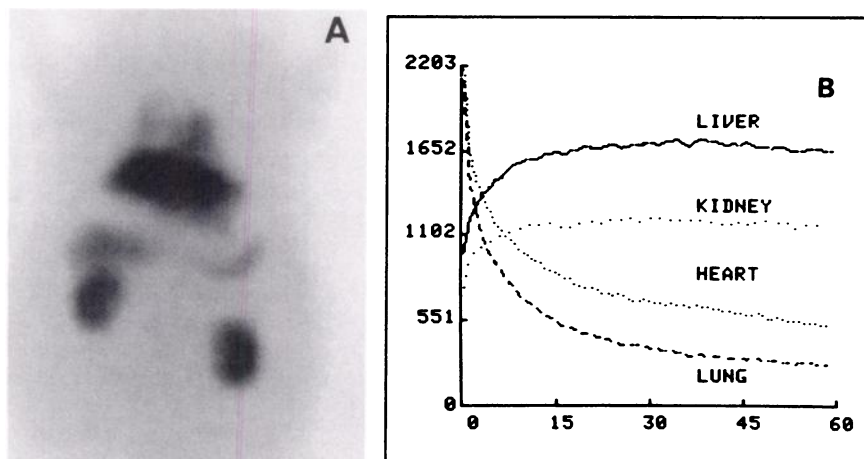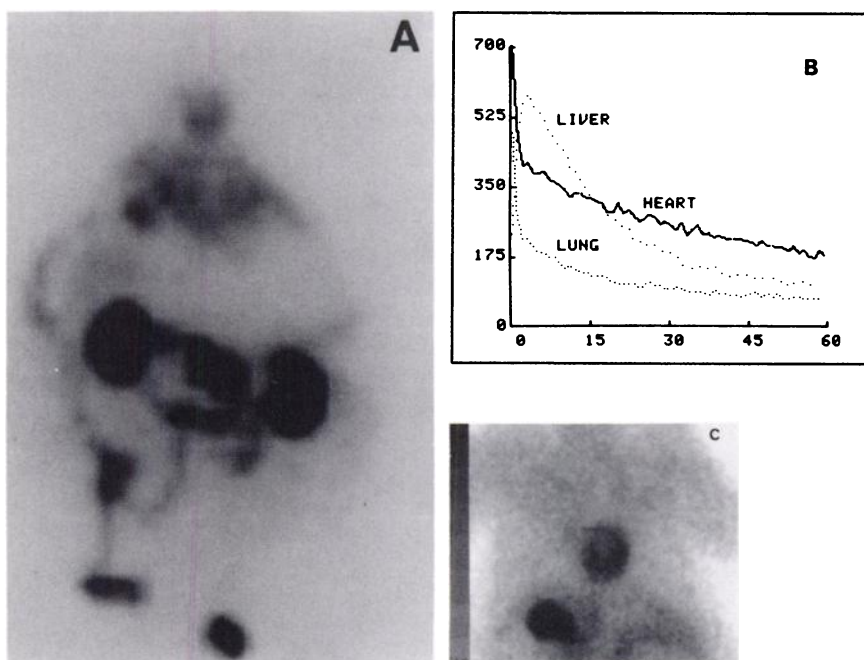
FIGURE 1. (A) Representative whole-body image of rabbit at 60-min postinjection of ^{99m}Tc-TBI (1.0 mCi). (B) Time-activity curves for fasted, anesthetized rabbit out to 60-min postinjection. Regions of interest are normalized to cpm/pixel.

which is an anterior view of the thoracic cavity of the rabbit at 60 min postinjection. Additionally, liver and kidney clearance, with half-times of 24 min and 16 min, respectively, were far more rapid than those of ^{99m}Tc-TBI. Consequently, the more rapid blood clearance and hepatobiliary excretion of ^{99m}Tc-CPI enhances the target-to-background ratios earlier in the study.

Quantitative biodistribution studies performed in the guinea pig at increasing times after intravenous injection of ^{99m}Tc-CPI confirmed 1.3% ± 0.3% of the injected dose localized in the heart at 5 min postinjection (Table 1). The heart activity gradually decreased over time to 0.19% ± 0.06% at 4 hr postinjection with a t$_{1/2}$ of 1.1 hr. The rapid clearance of background activity from blood and lung through high extraction by liver and kidney meets the requirements for a myocardial perfusion agent to assess induced transient ischemic events. Also, both rapid hepatobiliary and renal excretion were observed, which was in

concordance with the rabbit pharmacokinetic data. At times greater than 15 min after injection, the continued decrease in liver and kidney activity, without increase in blood concentration, indicates that hepatobiliary and renal excretion occurred without reabsorption.

A comparison of biodistribution data for ^{99m}Tc-CPI in four different species demonstrates a distinct variation in myocardial accumulation. Table 2 summarizes the biodistribution data for guinea pig, rat, mouse and chick at 5 min postinjection. For these early times after injection, the amount of ^{99m}Tc-CPI retained in the heart of guinea pig and chick was relatively high at 1.25% ± 0.32% and 1.33% ± 0.26% ID, respectively, which gave heart-to-lung ratios on a per gram basis of 2.4 and 1.8, also consistent with the rabbit images. However, for rat and mouse, the negligible activity in the heart (a factor of 20 less than that in guinea pigs) resulted in heart-to-lung ratios less than 1.0 with no possibility of myocardial visualization.

FIGURE 2. (A) Representative whole-body image of rabbit at 15-min postinjection of ^{99m}Tc-CPI (1.0 mCi). (B) Time-activity curves for fasted, anesthetized rabbit out to 60-min postinjection. Regions-of-interest are normalized to cpm/pixel. (C) High-resolution static 5-min acquisition of rabbit heart obtained at 60-min postinjection.

TABLE 1
Biodistribution of ^{99m}Tc-CPI in Guinea Pigs as %ID/Organ

Organ	5 min*	30 min*	60 min*	4 hr*
Heart	1.25 ± 0.32	1.11 ± 0.13	0.68 ± 0.04	0.19 ± 0.06
Blood	1.40 ± 0.27	0.92 ± 0.15	0.63 ± 0.10	0.30 ± 0.06
Lungs	0.91 ± 0.09	0.36 ± 0.04	0.10 ± 0.02	0.08 ± 0.02
Liver	13.3 ± 2.20	2.24 ± 0.82	1.21 ± 0.20	0.30 ± 0.04
Kidneys	10.4 ± 2.55	8.20 ± 1.81	5.12 ± 1.43	0.54 ± 0.22

* Mean of n ≥ 4 animals ± s.d. (σ − 1).

For guinea pig and chick, extraction and elimination of activity by the two major excretion routes were different from that in rat and mouse, with only 57.0% of the total activity excreted by 5 min in the former two species compared with 71.6% in the latter. This difference of biologic clearance rate does not appear to be due to more rapid blood clearance but to lower uptake of the agent in the muscle and fat of rat and mouse. The initial ratios of activity distributed between liver and kidney excretory pathways is not significantly different between the two groups of animals. At 5 min postinjection, 46.8% ± 5.6% and 10.3% ± 2.5% of the activity were in the hepatobiliary and renal clearance pathways, respectively, for guinea pig and chick compared with 59.5% ± 7.8% and 12.14% ± 4.4%, respectively, for mouse and rat.

As predicted from the biodistribution results, dynamic imaging studies in the guinea pig revealed good visualization of the heart by 5 min postinjection with heart-to-lung and heart-to-liver ratios of 2.0 and 1.1 after 30 min as shown in the time-activity curves (Fig. 3). The gamma camera images for the rat are strikingly different in that no delineation of the heart from the blood pool can be made. The liver clearance rates for both species were similar with a $t_{1/2}$ of 14 min.

Radiochemical Analysis of ^{99m}Tc-CPI In-Vitro Hydrolysis

Radiochromatographic analysis by HPLC of ^{99m}Tc-CPI after incubation at pH 10 for varying lengths of time resulted in the eventual observation of all nine hydrolysis species predicted for a rigid octahedral hexacoordinate complex as identified in Table 3. All the newly generated hydrolysis products were observed to have progressively shorter RP-HPLC retention times, indicating increasing hydrophilic character, as would be expected for the increasing number of deprotonated carboxylic acid groups on the newly generated complexes. Even the neutral monohydrolyzed product $[^{99m}$Tc(CPI)$_5$(H-CPI)]°, the first new species observed in the chromatograph, has a retention time shorter than the cationic ^{99m}Tc-CPI complex. The intramolecular separation of the cationic technetium(I) center from the terminal carboxylic acid, which is deprotonated at physiologic pH, produces a zwitterionic species with an overall neutral charge but yet more hydrophilic than the parent cation. Assignment of HPLC peak identities shown in Table 3 was made by comparison with characterized $[^{99}$Tc(CPI)$_6]^+$ hydrolysis products and measurement of peak integral ratios for juxtaposed species in the chromatograph to determine cis/trans and fac/mer geometric isomers based on a random sequential process as shown in Scheme 1 and described in detail elsewhere (10).

Incubation of ^{99m}Tc-CPI in rabbit plasma for 2 min at 37°C followed by HPLC analysis revealed 84% of the activity present as the original cationic agent with the remaining 16% consisting primarily of the monohydrolyzed neutral product. Similar low initial rates of in-vitro hydrolysis were observed after incubation in guinea pig and human serum with 93.3% ± 0.4% and 90.9% ± 1.0%, respectively, of ^{99m}Tc-CPI remaining after 2 min at 37°C. If incubation in these plasma samples is allowed to continue for longer periods of time, increased hydrolysis is observed with numerous species generated as exemplified in Figure 4 for the reaction in human serum after 40 min at 37°C. Control studies on the rate of decomposition by simple alkaline catalyzed hydrolysis in pH 7.4 buffered saline showed a significant but much slower rate of degradation. Table 4 contains the relative percent of each technetium compound present after incubation at 37°C

TABLE 2
Biodistribution of ^{99m}Tc-CPI in Four Species of Animal at Five Minutes Postinjection

	Guinea Pig		Rat		Mouse		Chick	
	%ID/organ	%ID/g	%ID/organ	%ID/g	%ID/organ	%ID/g	%ID/organ	%ID/g
Heart	1.25 ± 0.32	0.90 ± 0.20	0.066 ± 0.003	0.057 ± 0.002	0.046 ± 0.016	0.37 ± 0.19	1.33 ± 0.26	4.46 ± 1.28
Blood	1.40 ± 0.27	0.053 ± 0.008	3.82 ± 0.33	0.16 ± 0.018	2.16 ± 0.61	1.14 ± 0.42	—	1.83 ± 0.60
Lungs	0.91 ± 0.09	0.38 ± 0.11	0.25 ± 0.064	0.12 ± 0.015	0.23 ± 0.062	1.09 ± 0.45	1.03 ± 0.31	2.48 ± 0.64
Liver	13.3 ± 2.20	0.87 ± 0.29	20.0 ± 2.15	1.27 ± 0.11	11.5 ± 2.40	5.73 ± 1.10	21.9 ± 1.04	12.3 ± 1.40
Gut	34.4 ± 4.29	—	37.5 ± 5.72	—	50.0 ± 5.23	—	24.0 ± 3.78	—
Kidneys	10.4 ± 2.55	3.04 ± 0.78	2.71 ± 0.88	0.91 ± 0.27	1.37 ± 0.75	2.63 ± 1.18	5.79 ± 1.40	13.4 ± 4.35
Bladder	0.51 ± 0.35	—	9.30 ± 3.84	—	10.9 ± 3.35	—	3.84 ± 0.73	—
Spleen	0.58 ± 0.10	1.01 ± 0.23	0.048 ± 0.011	0.06 ± 0.007	0.048 ± 0.026	0.47 ± 0.15	0.30 ± 0.12	5.81 ± 2.92
Brain	0.029 ± 0.004	0.008 ± 0.001	0.015 ± 0.003	0.008 ± 0.001	0.045 ± 0.009	0.11 ± 0.026	0.048 ± 0.007	0.051 ± 0.004
Muscle	14.2 ± 4.50	0.079 ± 0.020	7.78 ± 1.63	0.049 ± 0.011	7.09 ± 3.41	0.57 ± 0.35	—	0.63 ± 0.17

* Mean of n ≥ 5 animals ± s.d. (σ − 1).
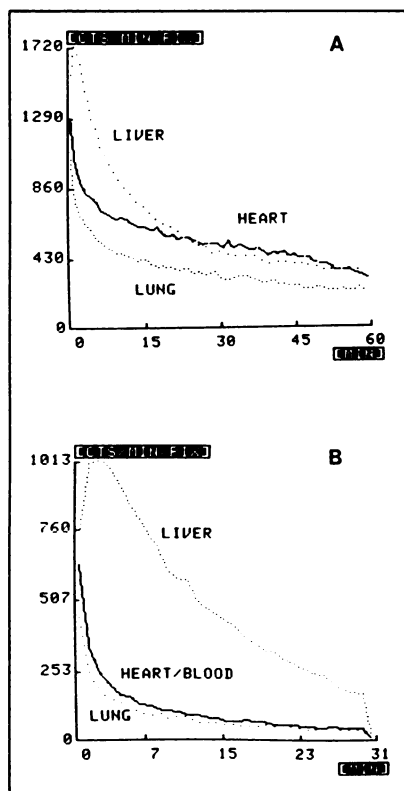
FIGURE 3. (A) Time-activity curves following intravenous injection of ^{99m}Tc-CPI (0.5 mCi) into fasted, anesthetized guinea pig out to 60-min postinjection. (B) Time-activity curves following intravenous injection of ^{99m}Tc-CPI (0.5 mCi) into fasted, anesthetized rat out to 30-min postinjection.

SCHEME 1. Distribution of products for sequential hydrolysis of a rigid octahedral hexacoordinate complex with ratios of geometric isomers predicted if hydrolysis occurs at random. Hydrolysis is shown as a continuation from the monohydrolyzed zwitterionic neutral compound.

a time as 10 sec, virtually only the dihydrolyzed species was present. Measurements at shorter time intervals showed that even after 3 sec at 25°C complete conversion of the cation of the neutral or anionic product had occurred (data not shown).

Not only does the rate of hydrolysis differ between these species but so does the ratio of geometric isomers observed for the metabolites of this octahedral complex. Figure 6 shows a comparison of the products obtained after incubation at 37°C for 2 min in rat plasma and 70 min in human plasma. Although the resolution of peaks is not
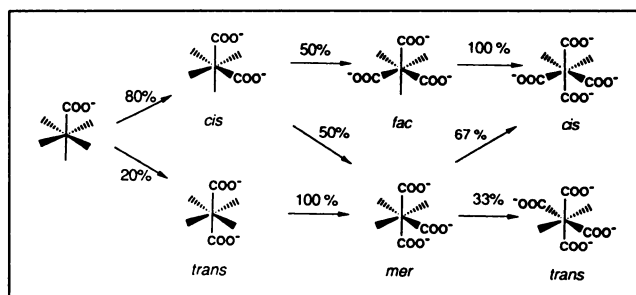
for 30 min in plasma from human, rabbit, guinea pig, rat and an aqueous solution buffered to pH 10. After these prolonged in-vitro incubation times, in no case did a significant amount of the parent cation remain.

A striking contrast was observed in the initial rate of hydrolysis and the ratio of products obtained after incubation of ^{99m}Tc-CPI with plasma from rat or mouse compared with the other species tested. Figure 5 compares the chromatographs obtained at 37°C after a 2-min incubation in human plasma and a 10-sec incubation in rat plasma. In human plasma, the radiochemical purity was similar to the control analysis. In rat plasma, however, after as short

TABLE 3
Reversed-Phase HPLC Analysis of ^{99m}Tc-CPI Hydrolysis Products

Peak elution order	k′	Identity
1	2.23	$[Tc(H\text{-}CPI)_6]^{-5}$
2	2.61	$[Tc(CPI)(H\text{-}CPI)_5]^{-4}$
3	2.81	$trans\text{-}[Tc(CPI)_2(H\text{-}CPI)_4]^{-3}$
4	2.94	$cis\text{-}[Tc(CPI)_2(H\text{-}CPI)_4]^{-3}$
5	3.14	$mer\text{-}[Tc(CPI)_3(H\text{-}CPI)_3]^{-2}$
6	3.25	$fac\text{-}[Tc(CPI)_3(H\text{-}CPI)_3]^{-2}$
7	3.34	$trans\text{-}[Tc(CPI)_4(H\text{-}CPI)_2]^{-1}$
8	3.46	$cis\text{-}[Tc(CPI)_4(H\text{-}CPI)_2]^{-1}$
9	3.68	$[Tc(CPI)_5(H\text{-}CPI)]^{0}$
10	4.20	$[Tc(CPI)_6]^{+}$

(CPI) = $CNC(CH_3)_2COOCH_3$, (H-CPI) = $CNC(CH_3)_2COO^-$.

FIGURE 4. Radiographic detection for HPLC analysis of ^{99m}Tc-CPI before (A) and after (B) in-vitro incubation with human serum for 40 min at 37°C.

TABLE 4
### Metabolites of ^{99m}Tc-CPI After Incubation in Plasma of Different Species at 37°C for 30 Minutes*

| Peak #	pH 10	Guinea Pig	Rabbit	Human	Rat
1	<0.5	<0.5	<0.5	<0.5	<0.5
2	2.4	2.8	<0.5	1.8	<0.5
3	2.6	11.2	1.9	2.1	<0.5
4	11.5	6.3	7.0	6.2	1.0
5	18.8	33.1	17.8	14.9	24.8
6	13.2	17.9	7.3	4.3	2.5
7	8.2	11.4	9.8	8.4	55.8
8	27.7	4.6	27.4	24.5	15.1
9	13.5	9.6	26.1	36.1	<0.5
10	2.1	3.1	2.7	1.7	<0.5

* Expressed as percent of activity present.

large, it can be seen that the first dihydrolyzed species eluted on this system ($trans$-[Tc(CPI)$_4$(H-CPI)$_2$]$^{-1}$) is present in much greater concentration in the rat plasma than the longer retained geometric isomer (cis-[Tc(CPI)$_4$(H-CPI)$_2$]$^{-1}$). By contrast, the longer retained cis isomer is present at four times the concentration of the $trans$-dihydrolyzed species following extended incubation in human plasma. The more rapid rate of metabolism and the alternate products produced indicate a completely different enzyme system in the blood of rat or mouse compared to the other species tested.

Biodistribution of [^{99m}Tc(CPI)$_5$(H-CPI)]°

Dynamic camera imaging of a rabbit following intravenous injection of [^{99m}Tc(CPI)$_5$(H-CPI)]° gave images strikingly different from those of the parent cationic agent (Fig. 7A). No heart activity is detectable in this 10-min image,
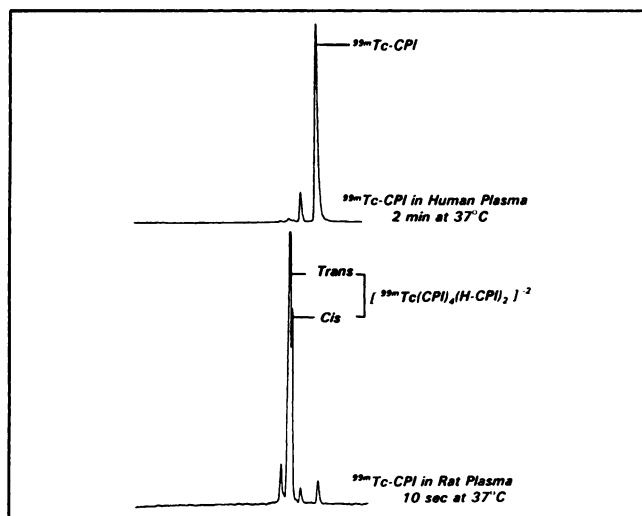
FIGURE 5. Radiographic detection for HPLC analysis of ^{99m}Tc-CPI following in-vitro incubation at 37°C in human plasma for 2 min showing the majority of radiolabel present as the cation and in rat plasma for 10 sec containing primarily the dihydrolyzed product.
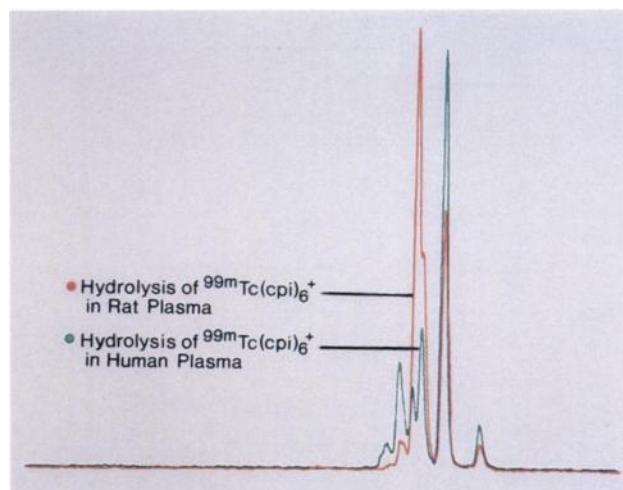
FIGURE 6. HPLC analysis of ^{99m}Tc-CPI following in-vitro incubation at 37°C for 70 min in human plasma and 2 min in rat plasma demonstrating formation of different ratios for cis and $trans$ geometric isomers of the dihydrolyzed metabolite.

which shows only liver, intestine and kidney distribution. The time-activity curves (Fig. 7B) indicate a consistent heart-to-lung ratio of 1.0 and a very rapid biliary clearance.

A comparison of biodistribution for the monohydrolyzed neutral species [^{99m}Tc(CPI)$_5$(H-CPI)]° with the parent cationic agent ^{99m}Tc-CPI in guinea pig at 5 min postinjection is presented in Table 5. The most significant difference between the two structurally similar compounds is that the percent of injected [^{99m}Tc(CPI)$_5$(H-CPI)]° activity retained in the heart is one-tenth that observed for the cationic ^{99m}Tc-CPI species. Also apparent is that the total activity excreted through the liver is slightly higher for the more hydrophilic monohydrolyzed species (57.7% ± 14.8%) than for the original ^{99m}Tc-CPI (47.7% ± 6.5%) with the concurrent inverse relationship observed for renal excretion, 2.3% ± 0.7% for the neutral compound versus 10.9% ± 2.9% for the cation. These mean values are the reverse of what one would expect on the basis of lipophilicity alone; consequently, overall charge must play a significant role on the rate of liver versus kidney extraction from the blood for these two compounds.

DISCUSSION

Biodistribution

Initial biologic screening of the technetium ester isonitrile complexes was performed in the rabbit because of its favorable predictive value with other potential heart agents (17). The 4–5 kg size of these animals is convenient for whole-body imaging on a gamma camera to obtain dynamic distribution with maximal resolution. In addition, the possibility of re-injecting the same animal, via the ear veins, minimizes intraspecies variation. Evaluation of biodistribution by dynamic gamma camera imaging, despite the drawback of limited quantitative data, allowed direct comparison of pharmacokinetics for different technetium
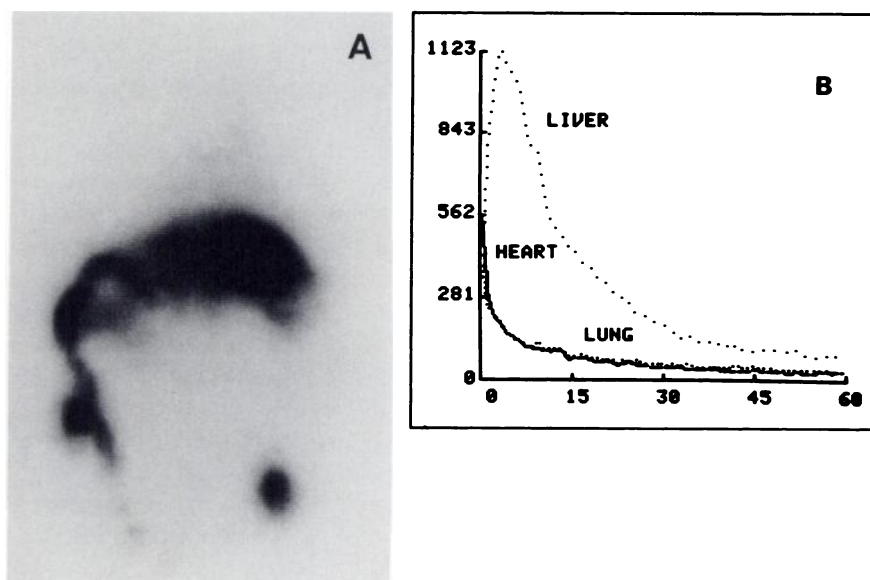
FIGURE 7. (A) Representative whole-body image of rabbit at 15-min postinjection of [^{99m}Tc(CPI)$_6$(H-CPI)]^0 (1.0 mCi), a monohydrolyzed metabolite of parent cationic agent. (B) Time-activity curves for fasted, anesthetized rabbit out to 60-min postinjection of [^{99m}Tc(CPI)$_6$(H-CPI)]^0. Regions of interest are normalized to cpm/pixel.

complexes. The more rapid clearance of activity from background organs to enhance target-to-nontarget ratios was the criterion for a second generation myocardial perfusion agent.

The guinea pig was chosen for initial quantitative biodistribution studies because of its critical predictive value in screening other cationic myocardial imaging agents (2). Heart accumulation of ^{99m}Tc-CPI has also been confirmed by imaging and modeling studies in dogs, pigs and primates (13) and by imaging studies in humans (18,19). The somewhat unusual inclusion of the chick in the interspecies comparison of biodistribution was to confirm the validity of using cultured chick myocytes for cellular kinetic studies (20). Thus far, the only species that have not shown myocardial uptake of ^{99m}Tc-CPI are rat and mouse. These two species do, however, show heart uptake for other technetium isonitrile compounds, including ^{99m}Tc-TBI and ^{99m}Tc-MIBI (11,21,22) and other cationic agents (23).

The choice of an "ideal" animal model depends upon the particular distribution property for which one is screen-ing, with the limitation that it be cost-effective. For the next generation heart agent, the debate centers around whether a higher extraction efficiency is critical for analyzing disease states and, if so, can it be obtained without increasing transient extraction by background organs, i.e., blood cells, lungs, systemic muscle or fat, that may gradually release the agent back into the bloodstream and interfere with acquiring the stress image. There appear to be two compartments to the uptake equation, a nonspecific component proportional to the lipophilicity of the complex and a membrane-specific component, which is more dependent upon molecular shape and charge distribution (24). For making comparisons of myocardial extraction of different compounds, a cell culture model offers the greatest control of conditions and variables. The examination of other properties that are prerequisites for a successful myocardial agent requires testing for blood interactions, preferably in human blood, and performing pharmacokinetic studies by dynamic imaging of medium sized animals, i.e., rabbit and guinea pig, and toxicity studies in the least expensive species available. In short,

TABLE 5
Biodistribution of ^{99m}Tc-CPI and [^{99m}Tc(CPI)$_6$(H-CPI)]^0 in Guinea Pigs at Five Minutes Postinjection

	[Tc(CN(CH₃)₂COOCH₃)₆]⁺		[Tc(CN(CH₃)₂COOCH₃)₆(CN(CH₃)₂COO⁻)]⁰	
	%ID/organ	%ID/gram	%ID/organ	%ID/gram
Heart	1.25 ± 0.32	0.90 ± 0.20	0.10 ± 0.02	0.065 ± 0.13
Blood	1.40 ± 0.27	0.053 ± 0.008	2.16 ± 0.93	0.074 ± 0.019
Lungs	0.91 ± 0.09	0.38 ± 0.11	0.252 ± 0.035	0.076 ± 0.014
Liver	13.3 ± 2.20	0.87 ± 0.29	9.11 ± 1.94	0.358 ± 0.086
Gut	34.4 ± 4.29	—	48.6 ± 12.9	—
Kidneys	10.4 ± 2.55	3.04 ± 0.78	2.12 ± 0.48	0.494 ± 0.146
Bladder	0.51 ± 0.35	—	0.176 ± 0.220	—
Spleen	0.58 ± 0.10	1.01 ± 0.23	0.056 ± 0.019	0.078 ± 0.031

* Mean of n = 6 animals ± s.d. (σ − 1).

there is no "ideal" model for the human and it is better to begin with the most optimistic system that gives the greatest number of potentially successful compounds.

As part of our initial screening for biologic properties, gamma camera images of rabbits injected with ^{99m}Tc-CPI were promising due to the early clear visualization of the heart. These images correlated with uptake studies in cultured avian myocytes (20) indicating a high extraction efficiency of ^{99m}Tc-CPI and agreed with the model of a freely diffusible cationic compound that was retained intracellularly by the high negative membrane potentials of myocytes and mitochondria (25). The absence of heart uptake in the biodistribution studies with rat and mouse was potentially contradictory to this general model of accumulation and raised doubts whether to proceed to human trials. Had initial screening of ^{99m}Tc-CPI been performed by biodistribution in the mouse, by far the least expensive mammalian species, its potential as a myocardial perfusion agent would have been missed. By contrast, the biodistribution and pharmacokinetics of ^{99m}Tc-CPI in rabbit and guinea pig indicate that this compound has optimal biologic behavior for a myocardial perfusion agent.

Radiopharmacology

The ^{99m}Tc-CPI complex can be easily produced in radiochemical yields ≥95% and is stable in solution at pH 4 to 7 for more than 24 hr. However, when diluted in physiological buffer at pH 7.4 or greater, significant hydrolysis is observed, as much as 38% in 1 hr. This rate of chemical decomposition or alkaline catalyzed hydrolysis is still much slower than that observed in human, rabbit or guinea pig serum with rates that are themselves almost 500 times slower than those observed in rat and mouse serum. The exceptionally rapid hydrolysis of ^{99m}Tc-CPI that occurs in rat and mouse serum and the absence of heart uptake of the monohydrolyzed species in either guinea pig or rabbit indicate that metabolism of the parent compound in the blood is the origin of the interspecies biodistribution differences. Additionally, an appreciation of how drastically the rate of esterase activity can vary between species suggests an explanation for the interspecies distribution differences observed with other compounds, such as the brain perfusion agent technetium N,N'-1,2-ethylenediyl-bis-L-cysteine diethyl ester (^{99m}Tc-ECD) (26).

The first product of hydrolysis, although still lipophilic with a net overall neutral charge, unlike other neutral complexes (27–29) does not accumulate significantly in the heart of guinea pig or rabbit and is not taken up in isolated cultured chick heart cells (30). If, as has been proposed, cationic isonitrile complexes are retained in myocytes in proportion to the plasma and mitochondrial membrane potentials (25), then a neutral compound would not be expected to be retained. Uptake of the neutral myocardial perfusion agent Cardiotec® by contrast appears to occur by a different mechanism, namely nonspecific

lipid partitioning (29). It should be noted that the lipophilic character of the neutral Cardiotec® agent is considerably greater than that of either ^{99m}Tc-CPI or its neutral monohydrolyzed product. This much greater lipophilicity is required for a neutral compound to be extracted efficiently by the heart and the absence of charge allows its rapid washout from myocardial tissue.

The fact that the neutral [[99m]Tc(CPI)₅(H-CPI)°], monohydrolyzed specie is not accumulated in guinea pig heart also suggests an explanation for the moderate myocardial washout of ^{99m}Tc-CPI observed in animals and in humans (31) in comparison to other isonitrile complexes (12,21, 32). Hydrolysis of a terminal ester group of ^{99m}Tc-CPI, after localization in guinea pig myocardial tissue, removes the cationic charge and allows diffusion out of the heart with the concentration gradient. This makes for an optimal agent because hydrolysis produces a radiolabel that clears from the heart and does not re-accumulate. It is not known whether the rate of hydrolysis after the cationic agent is in the heart is dominated by enzymatic or chemical hydrolysis.

CONCLUSION

Addition of the reactive methyl ester group to an isonitrile ligand followed by coordination to a reduced technetium central atom produces a lipophilic cationic complex that undergoes both base-catalyzed hydrolysis and enzymatic hydrolysis in vitro. The parent cationic ^{99m}Tc-CPI agent exhibits high initial uptake and retention in the myocardial tissue of rabbit, guinea pig and chick but virtually no accumulation in the heart of rat or mouse. The sequential metabolites of this agent are of increasingly hydrophilic character and negative charge, features which produce quite different biodistribution properties. Consequently, we conclude that rapid enzymatic hydrolysis of ^{99m}Tc-CPI in the blood of rat and mouse produces metabolites possessing a peripheral negative charge and lower lipophilicity, characteristics that inhibit their diffusion across the plasma membrane of heart tissue and retention based on a negative myocardial membrane potential.

REFERENCES

1. Gerundini P, Savi A, Gilardi MC, et al. Evaluation in dogs and humans of three potential technetium-99m myocardial perfusion agents. J Nucl Med 1986;27:409–416.
2. Ketring AR, Deutsch EA, Libson K, et al. The Noah's ark experiment. A search for a suitable animal model for the evaluation of cationic Tc-99m myocardial imaging agents. [Abstract]. J Nucl Med 1983;24:P9.
3. Edwards DS, Cheesman EH, Watson MW, et al. Synthesis and characterization of technetium and rhenium complexes of N,N'-1,2-ethylenediylbis-L-cysteine. Neurolite® and its metabolites. In: Nicolini M, Bandoli G, Mazzi U, eds. Technetium and rhenium in chemistry and nuclear medicine 3. Verona, Italy: Cortina International; 1990:433–444.

4. Tubergen K, Corlija M, Volkert WA, Holmes RA. Sensitivity of technetium-99m-d,l-HMPAO to radiolysis in aqueous solutions. *J Nucl Med* 1991;32:111–115.

5. Neirinckx RD, Burke JF, Harrison RC, et al. The retention mechanism of ^{99m}Tc-HMPAO: intracellular reaction with glutathione. *J Cereb Blood Flow Metab* 1988;8:4–12.

6. Sullivan DC, Silva JS, Cox CE, et al. Localization of ^{131}I labeled goat and primate anti-carcinoembryonic antigen (CEA) antibodies in patients with cancer. *Invest Radiol* 1982;17:350–355.

7. Thakur ML, DeFulvio J, Richard MD, Park CH. Technetium-99m labeled monoclonal antibodies: evaluation of reducing agents. *Nucl Med Biol* 1991; 18:227–233.

8. Walovich RC, Hill TC, Garrity ST, et al. Characterization of technetium-99m-L,L-ECD for brain perfusion imaging, part 1: pharmacology of technetium-99m-ECD in nonhuman primates. *J Nucl Med* 1989; 30:1892–1901.

9. Léveillé J, Demonceau G, De Roo M, et al. Characterization of technetium-99m-L,L-ECD for brain perfusion imaging, part 2: biodistribution and brain imaging in humans. *J Nucl Med* 1989;30:1902–1910.

10. Kronauge JF, Davison A, Roseberry A, Costello CE, Maleknia S, Jones AG. Synthesis and identification of the monocation, Tc(CNC(CH₃)₂COOCH₃)₆Cl, (Tc-CPI) and its hydrolysis products. *Inorg Chem* 1991;30:4265–4271.

11. Jones AG, Abrams MJ, Davison A, et al. Biological studies of a new class of technetium complexes: the hexakis (alkylisonitrile) technetium (I) cations. *Int J Nucl Med Biol* 1984;11:225–234.

12. Holman BL, Jones AG, Lister-James J, et al. A new Tc-99m-labeled myocardial imaging agent, hexakis(t-butylisonitrile)-technetium(I) [Tc-99m-TBI]: initial experience in the human. *J Nucl Med* 1984; 25:1350–1355.

13. Kronauge JF, Jones AG, Davidson A, Lister-James J, Williams SJ, Mousa SA. Isonitrile ester complexes of technetium [Abstract]. *J Nucl Med* 1986; 27:894A.

14. Kronauge JF, Davison A, Lister-James J, Noska MA, Jones AG. Interspecies comparison of the distribution of Tc-CPI [Abstract]. *J Nucl Med* 1987; 28:601A.

15. Abrams MA, Davison A, Jones AG, Costello CE, Pang H. Synthesis and characterization hexakis(alkyl isocyanide) and hexakis(aryl isocyanide) complexes of technetium(I). *Inorg Chem* 1983;22:2798–2800.

16. Jones AG, Davison A, LaTegola MR, et al. Chemical and in vivo studies of the anion oxo[N,N'-ethylenebis(2-mercaptoacetimido)]technetium(V). *J Nucl Med* 1982;23:801–809.

17. Eakins MN, Glavan KA, Kronauge JF, Neirinckx RD, LaTegola MR, Graff M. The myocardial uptake and biodistribution of kit formulated, ^{99m}Tc-labelled cationic complex, Tc(dmpe)₂Cl₂⁺. *Fourth Int Symp Radiopharmaceutical Chemistry, Jülich* 1982:186–188.

18. Holman BL, Sporn V, Jones AG, et al. Myocardial imaging with technetium-99m CPI: initial experience in the human. *J Nucl Med* 1987; 28:13–18.

19. Sporn V, Perez-Balino N, Holman BL, et al. Simultaneous measurement of ventricular function and myocardial perfusion using the technetium-99m isonitriles. *Clin Nucl Med* 1988;13:77–81.

20. Piwnica-Worms D, Kronauge JF, Holman BL, Lister-James J, Davison A, Jones AG. Hexakis(carbomethoxyisopropylisonitrile) technetium(I) [Tc-CPI]; a new myocardial perfusion agent: binding characteristics in cultured chick heart cells. *J Nucl Med* 1988;29:55–61.

21. Okada RD, Glover D, Gaffney T, Williams S. Myocardial kinetics of technetium-99m hexakis-2-methoxy-2-methylpropylisonitrile. *Circulation* 1988;77:491–498.

22. Meerdink DJ, Leppo JA. Comparison of hypoxia and ouabain effects on the myocardial uptake kinetics of technetium-99m hexakis 2-methoxyisobutyl isonitrile and thallium-201. *J Nucl Med* 1989;30:1500–1506.

23. Kelly JD, Higley B, Archer CM, et al. New functionalized diphosphine complexes of Tc-99m for myocardial perfusion imaging [Abstract]. *J Nucl Med* 1989;30:773.

24. Piwnica-Worms D, Kronauge JF, Delmon L, Holman BL, Marsh JD, Jones AG. Effect of metabolic inhibition on technetium-99m-MIBI kinetics in cultured chick myocardial cells. *J Nucl Med* 1990;31:464–472.

25. Piwnica-Worms D, Kronauge JF, Holman BL, Davison A, Jones AG. Comparative myocardial uptake characteristics of hexakis (alkylisonitrile) technetium (I) complexes: effect of lipophilicity. *Invest Radiol* 1989; 24:25–29.

26. Cheesman EH, Blanchette MA, Calabrese JC, et al. Technetium-99m complexes of ester derivatized diamine-dithiol ligands for imaging brain perfusion. *Seventh Int Symp Radiopharmaceutical Chemistry, Groningen* 1988:421–423.

27. Treher EN, Gougoutas J, Malley M, Nunn AD, Unger SE. New technetium radiopharmaceuticals: boronic acid adducts of vicinal dioxime complexes. *J Lab Compd Radiopharm* 1986:23:1118–1120.

28. Leppo JA, Meerdink DJ. Comparative myocardial extraction of two technetium-labeled BATO derivatives (SQ30217, SQ32014) and thallium. *J Nucl Med* 1990;31:67–74.

29. Kronauge JF, Chiu M, Cone JS, et al. Comparison of neutral and cationic myocardial perfusion agents: characteristics of accumulation in cultured cells. *Nucl Med Biol* 1992;19:141–148.

30. Piwnica-Worms D, Kronauge JF, Chiu ML. Uptake and retention of hexakis (2-methoxyisobutylisonitrile) technetium (I) in cultured chick myocardial cells: mitochondrial and plasma membrane potential dependence. *Circulation* 1990;82:1826–1838.

31. Sia STB, Holman BL, Campbell S, et al. The utilization of technetium-99m CPI as a myocardial perfusion imaging agent in exercise studies. *Clin Nucl Med* 1987;12:681–687.

32. Wackers FJ, Berman DS, Maddahi J, et al. Technetium-99m hexakis 2-methoxyisobutylisonitrile: human biodistribution, dosimetry, safety, and preliminary comparison to thallium-201 for myocardial perfusion imaging. *J Nucl Med* 1989;30:301–311.